

A finite-difference convective model for Jupiter's equatorial jet

Kwing L. Chan

Department of Mathematics, The Hong Kong University of Science and Technology
email: maklchan@ust.hk

Abstract. We present results of a numerical model for studying the dynamics of Jupiter's equatorial jet. The computed domain is a piece of spherical shell around the equator. The bulk of the region is convective, with a thin radiative layer at the top. The shell is spinning fast, with a Coriolis number = $\Omega L/V$ on the order of 50. A prominent super-rotating equatorial jet is generated, and secondary alternating jets appear in the higher latitudes. The roles of terms in the zonal momentum equation are analyzed. Since both the Reynolds number and the Taylor number are large, the viscous terms are small. The zonal momentum balance is primarily between the Coriolis and the Reynolds stress terms.

Keywords. Planets, hydrodynamics, numerical

Most of the early models for Jupiter's wind bands had the problem of not being able to generate a significant prograde jet at the equator. Calculations made by Christensen (2001) and Aurnou & Olson (2001) have changed the situation. Using a spectral approach to simulate incompressible convection in rotating shells, they have shown that dominant, prograde equatorial jets can be produced, if the Rayleigh number is high, the Eckman number is low, and the calculation is long enough in time. Here, we present preliminary results from a finite-difference model. The domain is limited to the equatorial and sub-tropics region. The finite difference code solves the fully compressible Navier-Stokes equation and the thermal equation for convection in a shell geometry. The restricted region makes it easier to resolve the hydrodynamics.

The calculation belongs to the Large Eddy Simulation category. The sub-grid-scale process is represented by a Smagorinsky viscosity and an associated thermal diffusivity; the turbulence Prandtl number is 1/3. The computed domain is a piece of spherical shell extending from 60 to 90 degrees in colatitude (θ), 0 to 80 degrees in longitude (ϕ), and 0.875 to 1 in radius (r). Here quantities are presented in units that make the top radius 1; the initial temperature, pressure, and density at top are also 1. The initial distribution contains two polytropic layers. The lower layer is convective, and the upper one is radiative (with Newton cooling); the boundary between the two is at the radius 0.975. The gas is taken to be ideal with a ratio of specific heats equal to 5/3. A constant energy flux of 0.0063 is uniformly applied at the bottom boundary. The upper, lower, and latitudinal boundaries are impenetrable and stress free. The longitudinal boundaries are periodic. The shell is spinning with an angular velocity (Ω) of 14. The finite difference code is similar to the one used by Robinson & Chan (2001); the mesh contains 200 (colatitude) x 722 (longitude) x 90 (radial) grid points.

After a long period of evolution (over 2 million time steps), the system is thermally relaxed. A prominent super-rotating equatorial jet is generated, and secondary alternating jets appear in higher latitudes (see Fig. 1). The resultant Coriolis number (= $\Omega L/V$; L is the total depth, V is a root-mean-square velocity) has the value 40 or 10, depending on whether V excludes or includes the mean flow. The effective Reynolds number is on

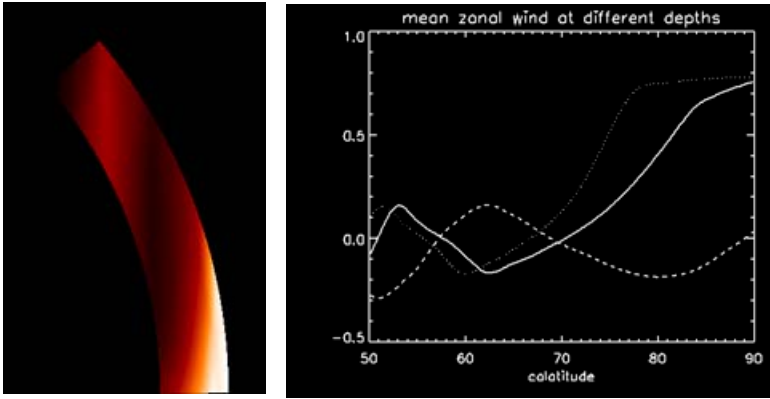


Figure 1. The left panel shows the distribution of the mean (longitudinally and temporally averaged) zonal velocity in the shell. Light (dark) colour shows prograde (retrograde) regions. The level contours of the zonal velocity are more or less parallel to the rotation axis, indicating the dominance of the Taylor-Proudman effect. A prograde jet is prominently displayed near the equator. The flow turns negative in a columnar region closer to the polar axis. Further towards the pole, a weak prograde column appears. The right panel shows the colatitudinal distributions of the mean zonal velocity at three height levels. The dotted, solid, and dashed curves are for the top of the box, the top of the convection zone, and the bottom of the box, respectively. Strong equatorial jets appear in the two upper levels. The equatorial jet is flanked by a significant retrograde jet. Going into the stable layer, the equatorial jet does not quickly vanish, but the peak at the equator turns flattened.

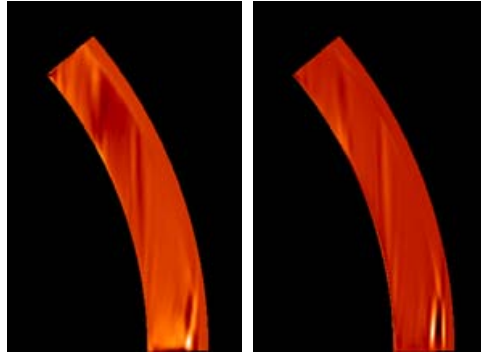


Figure 2. The left and right panels show the distributions of the divergence of the radial-zonal and colatitudinal-zonal components of the Reynolds stress (i.e. $\text{div}R_{r\phi}$ and $\text{div}R_{\theta\phi}$), respectively. Near the equator (excluding a narrow slit at the equator), the radial-zonal component is accelerating. In the secondary prograde region, the same term is decelerating. Some boundary effects can be seen near the bottom boundary and the convective-radiative interface.

the order of 700 or 3000, depending on the respective choice of V . The Taylor number ($= [4\Omega L^2/\nu]^2$; ν is the kinematic viscosity) is about 2×10^{11} .

The zonally and temporally averaged equation for angular momentum balance contains 6 action terms. Two are Coriolis terms associated separately with the radial and colatitudinal velocities (CV_r and CV_θ); two are divergence terms of the Reynolds stress ($\text{div}R_{r\phi}$ and $\text{div}R_{\theta\phi}$); the rest are two divergence terms of the viscous stress ($\text{div}S_{r\phi}$ and $\text{div}S_{\theta\phi}$). The left and right panels of Fig. 2 show the distributions of $\text{div}R_{r\phi}$ and $\text{div}R_{\theta\phi}$, respectively. The terms play different roles at different places. The distributions of the Coriolis and viscous stress terms (not shown) are similarly complicated.

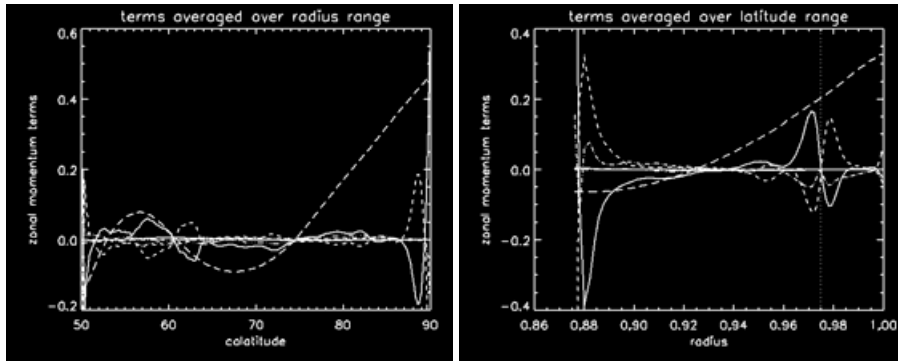


Figure 3. The left panel shows the colatitudinal distributions of the (radially) further averaged Coriolis (solid curves), Reynolds stress (short dashed), and viscous (dot-dashed) terms. Only the Coriolis term associated with the vertical velocity (CV_r) and the colatitudinal-zonal Reynolds stress term ($\text{div}R_{\theta\phi}$) are discernible as the other two terms are close to vanish after the averaging (as they should). The viscous terms are relatively small. The sum of the terms is shown by the double-dot-dashed curve. Since the sum should be in balance, this curve lies close to zero. The (radially) further averaged zonal velocity is shown by the long dashed curve; it shows a relationship with the locations where the roles of the Coriolis and Reynolds stress terms switch. The right panel shows the radial distributions of the (latitudinally) further averaged Coriolis (solid curves), Reynolds stress (short dashed), and viscous (dot-dashed) terms. The vertical dotted line shows the location of the convection-radiation interface (top of the convection zone). The Coriolis term associated with the colatitudinal velocity (CV_{θ}) and the radial-zonal Reynolds stress term ($\text{div}R_{r\phi}$) dominate the momentum balance. The radial-zonal viscous term ($\text{div}S_{r\phi}$) is small but not negligible. The other three terms are close to vanish after the averaging (as they should). The sum of all terms is shown by the double-dot-dashed curve; this line does lie close to zero. The (latitudinally) further averaged zonal velocity is shown by the long dashed curve. It shows that the mean rotation rate increases with radius.

To assist the analysis, the action terms are further averaged in two ways: one over the radial extent, and the other over the colatitudinal extent; the respective outcomes are then separately dependent on the latitude and the radius. The results are plotted in Fig. 3. In general, the viscous terms play minor roles. From the left panel, one can see that $\text{div}R_{\theta\phi}$ accelerates the equatorial jet but decelerates the prograde jet at the higher latitude. The actions are primarily balanced by those of the Coriolis term CV_r . From the right panel, one can see that $\text{div}R_{r\phi}$ decelerates the mean zonal flow in the top region of the convection zone and accelerates the flow in the bottom region. On the other hand, the Coriolis term CV_{θ} is doing the reverse.

In summary, zonal momentum balance is primarily between the Coriolis and Reynolds stress terms. These processes have exchanged roles in different regions.

Acknowledgements

This research is supported by the Hong Kong Research Grants Council under grant number HKUST600306

References

- Aurnou, J.M. & Olson, P.L. 2001, *Geophys. Res. Lett.* 28, 2557
 Christensen, U.R. 2001, *Geophys. Res. Lett.* 28, 2553
 Robinson, F.J. & Chan, K.L. 2001, *MNRAS* 321, 723